FERMILAB-PUB-81-088-E

PUB-81-088-E
3431

May
#439

UM HE 81-4

DIRECTOR'S OFFICE
MAR 17 1981

Experimental Test of the Drell-Yan Model in $p+W \rightarrow \mu^+ + \mu^- + X$

S.R.Smith, S. Childress, P.M.Mockett, J.P.Rutherfoord,

and R.W.Williams

University of Washington
Seattle, Washington 98195

H.R.Gustafson, L.W.Jones, M.J.Longo, T.J.Roberts, M.R.Whalley(a)

University of Michigan
Ann Arbor, Michigan 48109

D.A.Garelick, P.S.Gauthier(b), M.J.Glaubman, H.Johnstad(c),

M.L.Mallary(d), J.Moromisato, E.Pothier, and E. von Goeler

Northeastern University
Boston, Massachusetts 02115

W.P.Oliver

Tufts University
Medford, Massachusetts 02155

4 February, 1981
Submitted to
Physical Review Letters

PACS No. 13.60Hb

Abstract

We have measured the reaction $p+W \rightarrow \mu^{+}+\mu^{-}+X$ using a high intensity 400 GeV/c proton beam, a magnetized iron beam dump, and a wide acceptance detector. The μ-pair invariant mass spectrum contains 225,000 events above 6 GeV. Assuming the data near $x_F = 0$ is dominated by the Drell-Yan mechanism, we have extracted the nucleon sea quark distribution and find it to be a factor 1.6 ± 0.3 larger than that obtained by inelastic charged current neutrino scattering. We then compare the Drell-Yan prediction with our data over the full positive x_F region and find excellent agreement for a wide range of mass.

Hadronic production of dimuons with large invariant mass has contributed both to the discovery of quarkonium states and, via the Drell-Yan mechanism, to the elaboration of the quark-parton model. We report here results from continuum μ-pair production by 400 GeV/c protons at Fermilab. The experiment was characterized by high intensity and a very large acceptance which allow us to extract sea quark distributions which we use to test the Drell-Yan model in new kinematic regimes.

The apparatus has been described previously[1]; here we include only features particularly relevant to this measurement. A 400 GeV/c proton beam ($\sim 2\times 10^{11}$ protons per one second pulse) impinged on a 32 cm tungsten (W) target. Muons produced in the target penetrated 5.5 m of magnetized iron with a field of 2.15 T before reaching the detector. The detector consisted of two identical arrays of large solid angle placed symmetrically on the left and right sides of the beam direction. The position of these arrays with respect to the beam line direction could be varied. Each array contained two planes of crossed x-y hodoscope counters plus another smaller plane of "wedge" counters to reject low transverse momentum muons. Matrix logic circuits selected muons which projected back to the target in the non-bend (horizontal) plane and whose momenta, projected into the bend (vertical) plane, were above a predetermined threshold. In each array nine multiwire proportional chambers (MWPC's) with 2 mm wire spacing determined each muon straight line trajectory in the detector.

Data were recorded under three sets of conditions. Our lowest μ-pair invariant mass events were recorded with the two detector arrays as close to the beam line direction as possible and with no momentum cut in the matrix logic. The intermediate and high mass events were taken simultaneously with the detector arrays moved away from the beam line direction so that each array accepted muons whose laboratory angle was ≥ 18 mrad. The high mass events differed from the intermediate mass events in that the muons were required to pass the matrix logic momentum threshold and to trigger the optional "wedge" counter planes. The acceptances are exhibited in Fig. 1. For each set of conditions we recorded events in which the two arrays were triggered in time coincidence and also for events in which one array was out of time coincidence with the other. The various event types were prescaled at the trigger level, usually with high mass, in-time triggers given the greatest weight.

The small sample of like-charge pairs ($\mu^+\mu^+$ and $\mu^-\mu^-$) was used to make a background subtraction. We determined these to be dominated by accidentals by (1) comparing them to like-charge out-of-time yields, (2) observing that their yield rose linearly with intensity, and (3) direct calculation of in-time and out-of-time sources of such events. At no kinematic point was this correction greater than 10% of the signal.

Because the target was many hadronic absorption lengths thick, some of the secondary hadrons produced in the target also gave rise to μ-pairs. For most of the μ-pair invariant mass range of interest, this source was calculated to be ~30% of the continuum cross section at $x_F = 0$,[2] and to approach zero rapidly as x_F increased. Uncertainties in this correction are included in our quoted errors.

A Monte Carlo program was used to correct the data for acceptance. Such corrections are most uncertain where acceptance is changing rapidly. These critical regions have been checked by comparing results from the three trigger conditions in their two regions of overlap. We found agreement to better than 5%. Variations in detector efficiency were studied by comparing our results obtained at high intensity (where efficiency tended to be lower) with data obtained at low intensity. Again agreement was better than 5%.

The same Monte Carlo program was used to correct the μ-pair continuum for detector resolution effects including; (1) multiple Coulomb scattering of muons in the iron; (2) fluctuations in the energy loss of muons in the iron due to knock-ons, bremsstrahlung, and pair production; (3) finite target size and depth, and (4) MWPC position resolution. Radiative corrections[3] were made at the same time. The mass resolution function is Gaussian-like near its central value with an r.m.s. width of about 7.5% for masses from 5 to 15 GeV. The high mass side falls steeply while the low mass side has a long tail which, because of the steeply falling mass spectrum, proves to be of little consequence. Several checks of our calculated resolution contributions were made: (1) MWPC track fitting residuals, particularly the tails of the distributions, were carefully studied. (2) The track projection back to the target in the non-bend plane tested resolution contributions 1, 3, and 4. (3) The mass resolution function was compared with the shape of the peaks due to the ψ and Υ families. Remaining uncertainties due to imperfect knowledge of the resolution effects are taken into account in the errors quoted on our results.

Fig. 1 shows our fully corrected cross section plotted versus μ-pair invariant mass, q, for x_F between 0. and 0.2. The peak below 2.0 GeV is an unresolved mixture of contributions from μ-pair decays of ρ^0, ω, and ϕ and from the secondary gamma production of μ-pairs. The peak at 3.1 GeV is due to the ψ and the broad enhancement from 9 to 11 GeV is due to the Υ family.[4,5] There is no evidence for structure above 11 GeV. In extracting the cross section per nucleon from our measurements we assumed a nucleon number dependence for tungsten of the form

$$\frac{d\sigma/dq\,dx_F\,(pA\rightarrow\mu^+\mu^-X)}{d\sigma/dq\,dx_F\,(pN\rightarrow\mu^+\mu^-X)} = A^{\alpha} \qquad (1)$$

where α = 1.0 for $q>3.0$ GeV[6,7] and $\alpha = 0.7+q/10$ GeV for $0<q<3.0$ GeV[8]. We have also made a small correction for Fermi motion effects. An overall systematic error of 11% must be added to the data shown.

In the Drell-Yan model[9] the cross section for the hadronic production of massive lepton pair states is proportional to the weighted sum of products of the colliding hadrons' structure functions:

$$\frac{d\sigma}{dq^2\,dx_F} = \frac{K}{N_c}\,\frac{1}{s^2}\,\frac{4\pi\alpha^2}{3\tau^2}\,(x_F^2+4\tau)^{-1/2}\,G(x_A,x_B,q^2) \qquad (2)$$

$$G(x_A,x_B,q^2) = \sum_i e_i^2\{x_A f_i^A(x_A,q^2)\,x_B\bar{f}_i^B(x_B,q^2)+x_A\bar{f}_i^A(x_A,q^2)\,x_B f_i^B(x_B,q^2)\}$$

where the sum on i extends over all quark flavors and e_i is the fractional quark charge. The structure functions, $f_i(x,q^2)$, are the same scale breaking structure functions used in deep inelastic lepton scattering[10]. In the case of a proton beam (hadron A) on a tungsten target (hadron B is 40% proton and 60% neutron) the structure functions are constrained by the deep inelastic lepton scattering data. N_c (=3) is the number of quark colors and K is a factor which is unity in the naive Drell-Yan model. It is included to account for the QCD corrections to Eq. (2) which, to lowest order, are responsible for roughly a factor of 2 in the cross section, nearly independent of the kinematics.[11]

Following the work of others[6,12-15] we have extracted the nucleon sea quark distribution under the assumption that the Drell-Yan model is correct by using

$$F_2(x,q^2) = \sum_i e_i^2\{xf_i(x,q^2)+x\bar{f}_i(x,q^2)\} \qquad (3)$$

from charged lepton scattering data[16] and our μ-pair cross section of Fig. 1 above 5 GeV but excluding the Υ region. Because these data are near $x_F = 0$ the quark momentum fractions are constrained so that $x_A \simeq x_B \equiv x$ and therefore $q^2 \simeq x^2 s$.

Thus any scale breaking q^2 dependence of the sea is absorbed into the x dependence in this method.

Two different parameterizations for the nucleon sea-quark distribution have been employed[12,13]. In the first, referred to as the symmetric sea, $x\bar{f}_u(x) = x\bar{f}_d(x) = a(1-x)^b$ where a and b are fitting parameters. In the second, referred to as the asymmetric sea,[17] $x\bar{f}_d(x) = a(1-x)^b$ and $\bar{f}_u(x) = (1-x)^{2.5}\bar{f}_d(x)$. In both cases $f_s(x) = \bar{f}_s(x) = [\bar{f}_u(x)+\bar{f}_d(x)]/4$ and we neglect all higher mass quarks. For $F_2(x,q^2)$ we use the parameterization of T. Kirk[16,18] where for q^2 we use the square of the μ-pair invariant mass (as our notation implies) ignoring the sign change in going from the space-like to the time-like domain[10,15]. We assume that $F_2^n(x)/F_2^p(x)$ is q^2 independent and is given by $0.807 - 0.535x$.[13,19] For the symmetric sea we find $a = 0.46 \pm 0.03 \pm 0.06$, $b = 8.2 \pm 0.2 \pm 0.3$ while for the asymmetric sea $a = 0.50 \pm 0.03 \pm 0.06$, $b = 7.4 \pm 0.2 \pm 0.3$ where the first error is statistical and the second is systematic. We note that if we had allowed our sea quark distributions to have a q^2 dependence as predicted by QCD[20,21] then in both fits the exponent, b, would be smaller.

We compared our nucleon sea with that obtained in neutrino-nucleon deep inelastic charged current scattering by the CDHS collaboration[22] who obtained[15,21] $x\bar{f}_u(x)+x\bar{f}_d(x) = 0.36(1-x)^{6.5}$ for $0<x<0.3$. Our sea parameterizations cover the range $0.18<x<0.58$ and so there is only a narrow region of overlap. In this region we find that our sea is substantially larger than theirs suggesting that the factor in Eq. (2) should be $K = 1.6 \pm 0.3$ consistent with the calculation of Ref. 11. The difference in exponents may be due to scaling violations[21].

To test the Drell-Yan model we have compared the predictions of Eq. (2) with our data which covers a much wider combined range of x_F' and q. Fig. 2 shows our data at several different values of q graphed versus x_F'. The curves are the predictions of the asymmetric sea fit. The agreement is quite good over several orders of magnitude in cross section. The small deviations may be due to the scale violations in the sea which we have ignored here. This excellent agreement with the model suggests that the continuum is dominated by the Drell-Yan mechanism over the full range of kinematics explored here.

We gratefully acknowledge the assistance of the following people at various stages of the experiment: H. Haggerty, R. Tokarek, E. King, G. Hicks, J. Gallagher, D. Logothetis, E. Kaiser, R. Shoemaker, T. Toohig, C. N. Brown, C. McGuire, P. Czarapata, D. Hinds, J. Hanson, F. Toevs, D. Forbush, N. Ward, H. Schick, D. Wallen, and R. Weinstein. This work was supported by the National Science Foundation and the Department of Energy.

Footnotes and References

(a) Now at Department of Physics, University of Sheffield, Sheffield, England

(b) Now at American Science and Engineering, Cambridge, MA 02139

(c) Now at Fermilab, Batavia, IL 60510.

(d) Now at Digital Equipment Corporation, 146 Main Street, Maynard, MA 01754

1 D. A. Garelick et al., Phys. Rev. D18, 945 (1978).

2 We use standard definitions of kinematic variables; q is the invariant mass of the μ-pair, p_L is the longitudinal momentum of the μ-pair in the hadronic center-of-mass, and s is the square of the hadronic center-of-mass energy. From these are defined; $x_F = 2p_L/\sqrt{s}$ and $\tau = q^2/s$. In the Drell-Yan picture, a quark (antiquark) in hadron A annihilates an antiquark (quark) in hadron B. The fraction of the momentum of hadron A (B) carried by the interacting quark (antiquark) is x_A (x_B). It can be shown that $x_A x_B = \tau$ and $x_A - x_B = x_F$. For binning data it is more appropriate to use $x_F' = x_F/(1-\tau)$.

3 A. Soni, Phys. Rev. D8, 2264 (1973).

4 S. W. Herb et al.,Phys. Rev. Lett. 39, 252 (1977).

5 K. Ueno et al., Phys. Rev. Lett. 42, 486 (1979).

6 D. M. Kaplan et al., Phys. Rev. Lett. 40, 435 (1978).

7 L. M. Lederman, in Proceedings of the 19th International Conference on High Energy Physics, Tokyo, August 23-30, 1978, edited by S. Homma, M. Kawaguchi, and M. Miyazawa (Physical Society of Japan, Tokyo, 1979), p. 706.

8 K. J. Anderson et al., Phys. Rev. Lett. 42, 944 (1979).

9 S. Drell and T.-M. Yan, Phys. Rev. Lett. 25, 316 (1970); Ann. Phys. 66, 578 (1971); G. R. Farrar, Nucl. Phys. B77, 429 (1974).

10 R. K. Ellis, H. Georgi, M. Machecek, H. D. Politzer, and G. G. Ross, Phys. Lett. 78B, 281 (1978); D. Amati, R. Petronzio, G. Veneziano, Nucl. Phys. B140, 54 (1978).

11 G. Altarelli, R. K. Ellis, and G. Martinelli, Nucl. Phys. B157, 461 (1979).

12 Private communications with W. Innes, A. S. Ito, C. N. Brown, and L. M. Lederman are gratefully acknowledged.

13 A. S. Ito et al., FERMILAB-Pub-80/19-EXP (1980) Submitted to Phys. Rev. D.

14 V. Barger and R. J. N. Phillips, Phys. Lett. 73B, 91 (1978).

15 E. L. Berger, in AIP Conference Proceedings, No. 45, Particles and Fields Subseries No. 14, New Results in High Energy Physics - 1978 (Vanderbilt Conference), edited by R. S. Panvini and S. E. Csorna (American Institute of Physics, N. Y., 1978), p. 178; E. L. Berger, in Orbis Scientiae, High Energy Physics in the Einstein Centinnial Year, edited by A. Perlmutter, F. Krausz, and L. F. Scott (Plenum, New York, 1979), p. 455.

16 B. A. Gordon et al., Phys. Rev. D20, 2645 (1979).

17 Suggested by R. D. Field and R. P. Feynman, Phys. Rev. D15, 2590 (1977) and by the generalized Adler sum rule. See A. P. Contogouris and S. Papadopoulos, Hadronic Journal 1, 504 (1978).

18 T. B. W. Kirk, Fermilab Report No. TM-791 (1978).

19 W. B. Atwood, Ph.D. thesis, Stanford University, SLAC Report 185 (1975); A. Bodek et al., Phys. Rev. D20, 1471 (1979).

20 G. Altarelli and G. Parisi, Nucl. Phys. B126, 298 (1977).

21 R. Stroynowski, Lectures an the SLAC Summer Institute on Particle Physics: Quantum Chromodynamics at Stanford, California, July 9-20, 1979; SLAC-PUB-2402 (1979).

22 J. G. H. de Groot et al., Zeitschrift fur Physik C1, 143 (1979).

23 J. Badier et al., Phys. Lett. 89B, 145 (1979); M. A. Abolins et al., Phys. Lett. 82B, 145 (1979); R. Barate et al., Phys. Rev. Lett. 43, 1541 (1979).

Figure Captions

1. μ-pair production cross section at $x_F' = 0.1$ as a function of μ-pair invariant mass, q. The curve through the data is the result of the asymmetric sea fit described in the text. The thickness of the curve indicates systematic errors in the data which are mass dependent. An overall systematic error of 11% is not shown. The acceptance functions use the scale at the right. The letters indicate (a) low, (b) intermediate, and (c) high mass trigger acceptances. The inset shows our continuum-subtracted data in the region of the Υ family on a linear scale.

2. μ-pair production cross sections as a function of c.m. longitudinal momentum fraction, x_F'. The curves are predictions using the asymmetric sea described in the text. The fine lines indicate the range of systematic errors in the data which vary with the kinematics.

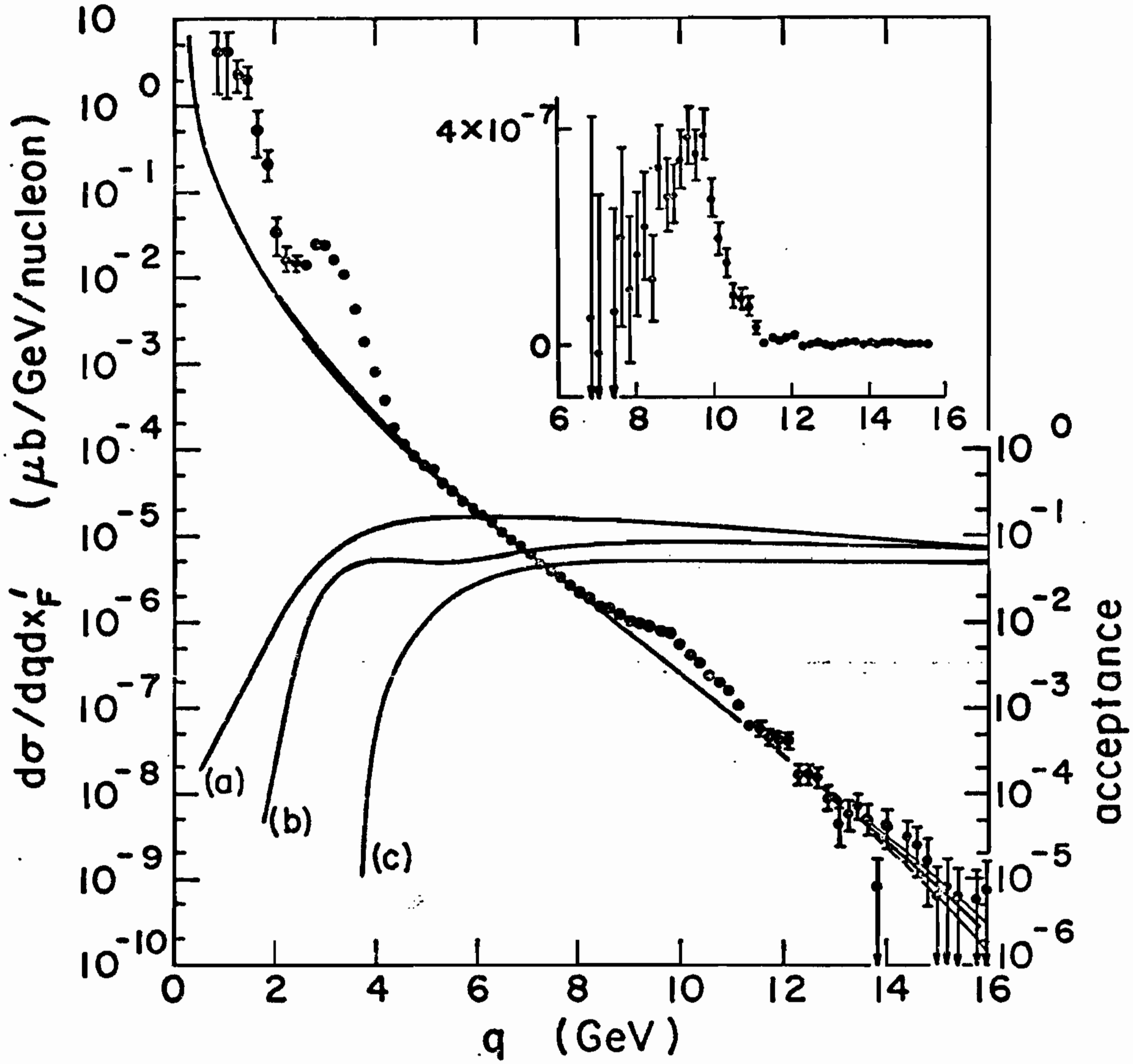

$d\sigma/dq dx'_F$ (μb/GeV/nucleon)
10
10^0
10^{-1}
10^{-2}
10^{-3}
10^{-4}
10^{-5}
10^{-6}
10^{-7}
10^{-8}
10^{-9}
10^{-10}
acceptance
10^0
10^{-1}
10^{-2}
10^{-3}
10^{-4}
10^{-5}
10^{-6}
(a)
(b)
(c)
4×10^{-7}
0
6
8
10
12
14
16
0
2
4
6
8
10
12
14
16
q (GeV)

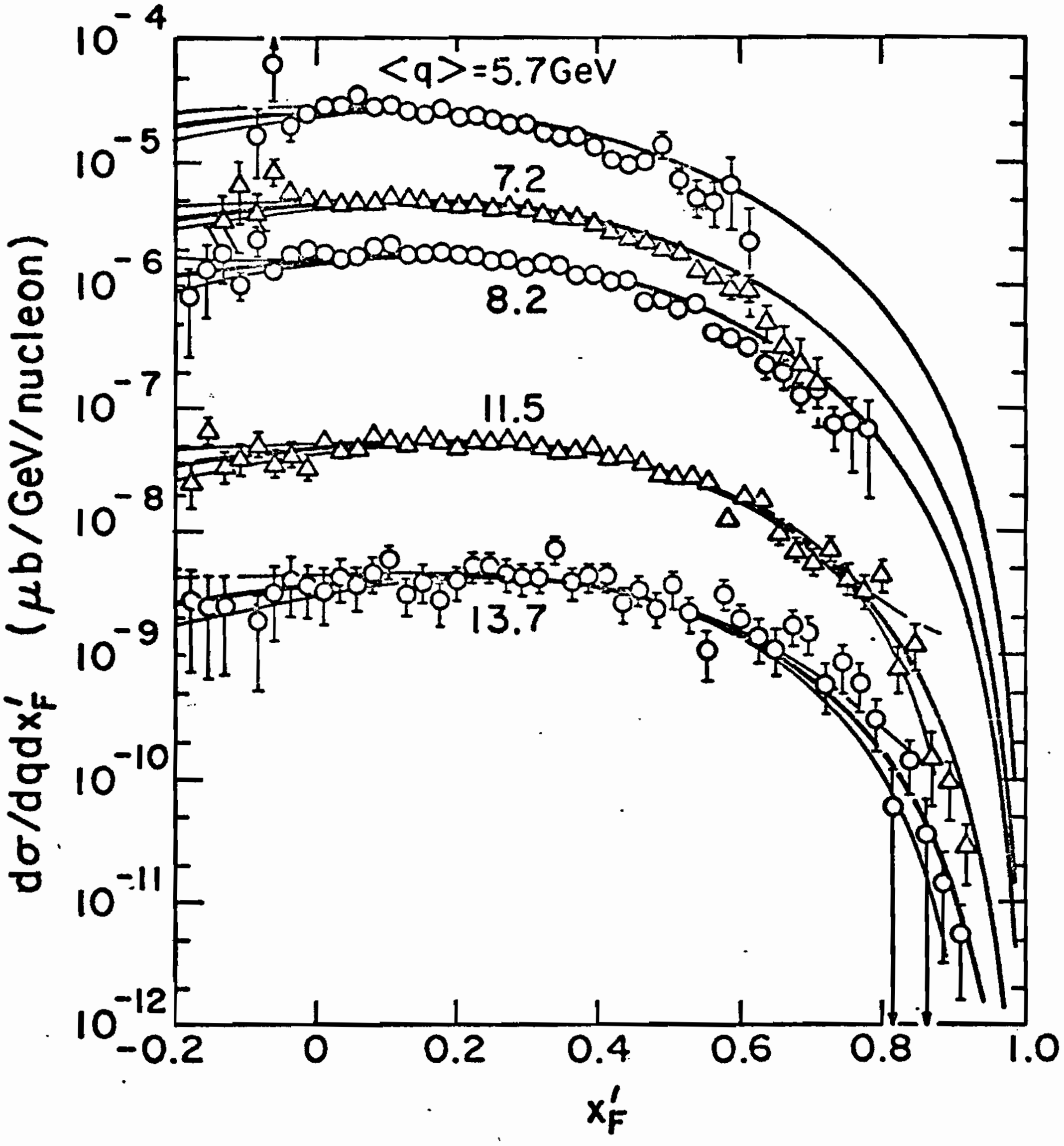

10^-4
10^-5
10^-6
10^-7
10^-8
10^-9
10^-10
10^-11
10^-12
-0.2
0
0.2
0.4
0.6
0.8
1.0
x'_F
dσ/dqdx'_F (μb/GeV/nucleon)
<q>=5.7GeV
7.2
8.2
11.5
13.7